Nanostructures

DOI: 10.1002/anie.201301199

Synthesis of Enantiopure Carbonaceous Nanotubes with Optical Activity**

*Shaohua Liu, Yingying Duan, Xuejiao Feng, Jun Yang, and Shunai Che**

Chirality and the related optical activity are abundant in nature and fascinating properties of many molecules and biomolecules. Recently, chiral inorganic materials have attracted great attention because of their potential applications, for example, in chiral separations, chemical and biological sensors, and optical devices.[1] Carbon-based materials, such as carbon nanotubes (CNTs) and graphene as well as their composites, have aroused continual and tremendous interest because of their high electrical conductivity, strength, flexibility, and their light weight.[2] Chiral carbon-based nanotubes with helical structures and high specific surface areas are promising one-dimensional nanomaterials because of their superior electronic, mechanical, and thermal properties. As expected, they have been useful in asymmetric catalysis,[3] induction of chirality in nanostructures,[4] and sensing of chiral molecules.[5]

However, selective synthesis of enantiopure chiral carbon-based nanotubes with optical activity is still a formidable challenge that remains unsolved. Most of the CNTs that are grown by chemical vapor deposition are mixtures of equal amounts of left- and right-handed helical structures, which as a whole do not have optical activity.[6] To obtain enantiopure chiral CNTs with optical activity, it is essential to enrich and separate racemic mixtures through so-called enantioenrichment. Generally, this involves multiple steps, including the controlled synthesis of CNTs and the elaborate selection and removal of guest molecules.[7] Although single-handed helical CNTs can be obtained in slight excess using a solid-supported Co–Mo catalyst in a one-step selective synthesis, the reason for this excess is still not clear, and their optical activity has also not been explored.[6b,8]

Herein, we report a one-step synthesis of enantiopure chiral carbonaceous nanotubes (CCNTs) by carbonization of self-assembled chiral polypyrrole (CPPy) nanotubes. The CPPy nanotubes were templated by self-assembly of enantiopure chiral amphiphilic N-acylamino acid molecules and subsequent polymerization of the bound pyrroles.[9] These CPPy nanotubes and their carbonized products gave enantiopure materials with distinct and robust optical activity, which could be attributed to the ordered helical arrangement of the polymers or carbon nanostructures. Their enantiomeric materials showed the mirror-imaged CD signals.

So far, soft-template-directed self-assembly has not been used to direct the surface deposition of a carbon source to form a template–carbon complex, because the required interaction between the template and the carbon source is extremely difficult to achieve. Our approach is based on the formation of CPPy nanotubes as a result of electrostatic interactions between the carboxylic amphiphilic molecules and the pyrrole monomers,[9] and subsequent carbonization. It is well known that lipid amphiphilic molecules, such as N-acylamino acids and fatty acids with hydrophobic alkyl chains, can self-assemble to form helical ribbons or fibers with a bilayered molecular arrangement (Scheme 1),[10] which can

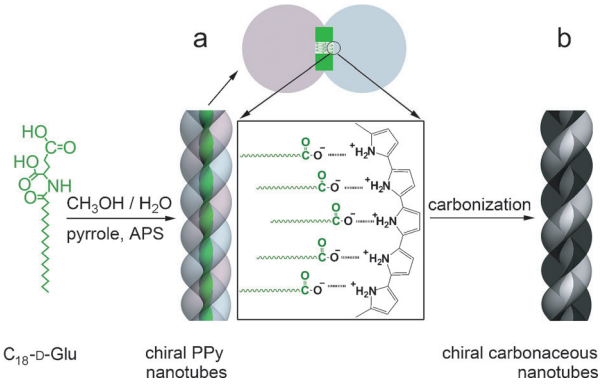

Scheme 1. Illustration of the synthesis of CPPy nanotubes and CCNTs. a) CPPy nanotubes prepared by self-assembly of C_{18}-D-Glu (template) with ammonium persulfate (APS) as initiator. b) CCNTs prepared by carbonization of CPPy nanotubes under an Ar atmosphere.

be used as templates for the oriented polymerization of pyrrole monomers through electrostatic interactions between the negatively charged carboxylic acid heads and the positively charged imine nitrogen atoms. Left- and right-handed chiral PPy (L-CPPy and R-CPPy) nanotubes can be prepared by using surfactants derived from L- and D-glutamic acid, respectively.[9] The preferential interaction, which occurs on both sides of the above-mentioned helical ribbon (one side shown in Scheme 1, enlarged section), leads to the formation of double-helical PPy nanotubes.[10b] After calcination under an inert atmosphere at different temperatures, such CPPy nanotubes can be carbonized to the carbon-based materials with well-maintained helical morphology. The left- and right-handed CCNTs were denoted as L-CCNT and R-CCNT, respectively.

[*] S. Liu, Y. Duan, X. Feng, Prof. J. Yang, Prof. S. Che
School of Chemistry and Chemical Engineering, State Key Laboratory of Metal Matrix Composites, Shanghai Jiao Tong University
800 Dongchuan Road, Shanghai, 200240 (P.R. China)
E-mail: chesa@sjtu.edu.cn
Homepage: http://che.sjtu.edu.cn

[**] This work was supported by the 973 project (2009CB930403) of China and Evonik Industry.

Supporting information for this article is available on the WWW under http://dx.doi.org/10.1002/anie.201301199.

Figure 1 shows scanning electron microscopy (SEM; a–c) and high-resolution transmittance electron microscopy (HRTEM; d–f) images of the CPPy nanotubes templated by *N*-stearyl-D-glutamic acid (C_{18}-D-Glu), and CCNTs carbonized at 550 °C (CCNTs-550) and 950 °C (CCNTs-950). These samples are composed exclusively of right-handed double-helical fibers with uniform morphology. The wider surface of the helical ribbon would attract more monomer molecules of PPy to polymerize on them, resulting in the formation of double-helical PPy nanotubes as mentioned above. The outer diameters of the as-prepared CPPy nanotubes are in the range of 70–100 nm and the pitches of outer surface along the rod axis are estimated to be all about 250 nm, as indicated by black arrows. After carbonization under an Ar atmosphere, the outer diameters of the nanotubes were slightly decreased and their surface became gradually folded with increasing temperature. However, the double-helical morphology of the nanotubes was still well-maintained, even after carbonization at high temperatures (e.g., 950 °C), thus displaying their high ability to memorize the original morphology. When the C_{18}-L-Glu was used as template, the resulting products displayed the same morphology but with the opposite helicity (see Figure S1 in the Supporting Information).

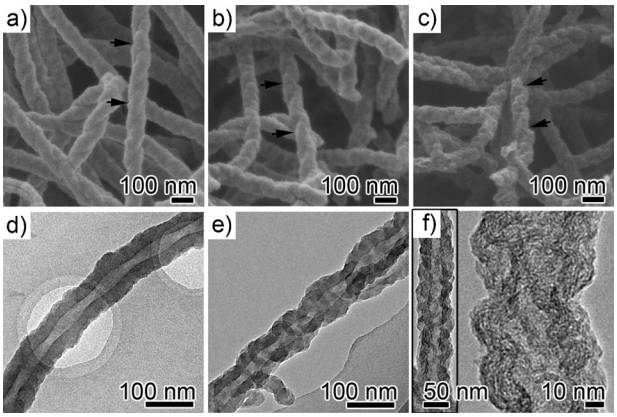

Figure 1. SEM (a–c) and TEM images (d–f) of the R-CPPy nanotubes (a, d), R-CCNTs-550 (b, e), and R-CCNTs-950 (c, f).

The HRTEM images in Figure 1 d–f indicate that the CPPy nanotubes possess helical inner tubes with a diameter of approximately 25 nm. After carbonization under Ar atmosphere, the CCNTs-550 showed no obvious change in morphology compared to CPPy nanotubes. HRTEM images of CCNTs-950 showed a layered arrangement, which may be the characteristic structure of graphitized carbon. Similarly, previous reports have shown that PPy materials can be carbonized to graphitized structures by dehydrogenation and growth of PPy chains, and rearrangement of carbon atoms in these chains.[11] CCNTs could thus be regarded as helically arranged carbonaceous nanostructured building blocks (CNBBs) consisting of graphitic and amorphous carbon.

The N_2 adsorption–desorption isotherms (see Figure S2 and Table S1 in the Supporting Information) of CPPy nanotubes and CCNTs-550 show a large Brunauer–Emmett–Teller (BET) surface area of more than 130 $m^2 g^{-1}$, and a pore size of about 25 nm. However, the specific surface area and pore size of CCNTs-950 are slightly smaller, which could be attributed to the pyrolysis of organic components during graphitization.

The chemical compositions of these samples were analyzed by X-ray photoelectron spectroscopy (XPS; Figure 2; for detailed data see Table S2 in the Supporting Information). The nitrogen atoms in CPPy nanotubes exist as pyrrolic nitrogen at 400 eV, which gradually transforms to pyridinic nitrogen at 398 eV, and graphitic nitrogen at 401 eV. After carbonization at 950 °C, the nitrogen atoms exist mostly as graphitic nitrogen, which indicates that the degree of graphitization deepened with increasing carbonization temperature,[11a,12] while the nitrogen content gradually decreased. Furthermore, these results show that N-doped carbon nanotubes (CN_x) were obtained by carbonization of CPPy nanotubes at 550–950 °C. The introduction of nitrogen atoms into CCNTs could create more active sites for anchoring functional metal nanoparticles, such as Pt and Ag, thus resulting in the use of CCNTs as, for example, novel supports of catalysts for direct methanol fuel cells (DMFC), bactericides, and sensors.[11a,13]

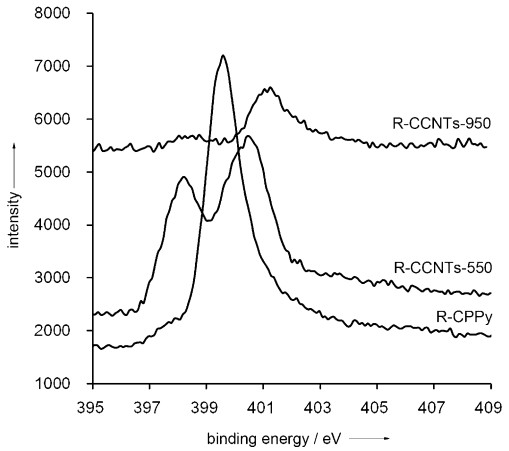

Figure 2. N1s XPS spectra of R-CPPy nanotubes, R-CCNTs-550, and CCNTs-950.

The chemical compositions of the CPPy nanotubes before and after carbonization were further examined by FT-IR spectroscopy (see Figure S3 in the Supporting Information). The spectra show no distinct bands at around 2840 and 2920 cm^{-1} (corresponding to CH_2/CH_3 stretching vibration of C_{18}-L/D-Glu) in the as-prepared samples, probably because the lipid molecules are completely enclosed in this system.[9] The characteristic stretching vibration bands of pyrrole rings at 1549 and 1470 cm^{-1}, and the bands characteristic for stretching of conjugated C-N and planar C-H at 1302 and 1040 cm^{-1}, respectively, demonstrate the formation of PPy.[9,11a,14] However, the above-mentioned characteristic bands become weaker and finally completely disappear with increasing carbonization temperature, thus indicating that CPPy nanotubes are converted to all-carbon materials at 950 °C. This conversion was further confirmed by ^{13}C NMR spectroscopy (Figure S4 in the Supporting Information). The

^{13}C NMR spectra of CPPy nanotubes and R-CCNTs-550 show a common resonance at about 128 ppm, suggesting that both of them predominantly feature α–α′ bonding.[15] However, no such signal was found in the spectra of R-CCNTs-950, thus indicating that after carbonization at 950 °C, hydrogen was completely eliminated and the CPPy nanotubes were converted to all-carbon materials.

The microstructures were also investigated using XRD and Raman spectroscopy (see Figures S5 and S6 in the Supporting Information). The XRD curves show only a broad maximum at approximately 23.6°, corresponding to the intermolecular π–π interaction of PPy chains similar to that of aromatic groups.[11a,14b] After carbonization, the maximum was increased in intensity and shifted to a wider angle (around 25.2°), which is characteristic of the (002) plane in graphite. Moreover, a weak maximum at 43.4° corresponds to the (100) plane in graphite, the presence of which might be attributed to the graphitization of the CPPy nanotubes. Raman spectra of the CPPy samples show a characteristic band at around 1556 cm^{-1}, corresponding to sp^2-hybridized carbon atoms (C=C), which gradually shifts to a higher wavenumber of around 1583 cm^{-1} after carbonization at 950 °C. The band at 1583 cm^{-1}, corresponding to a graphitic species (G-band), may be ascribed to the graphite structure of carbon atoms.[11b,16] In addition, the characteristic band at around 1346 cm^{-1}, corresponding to sp^3-hybridized carbon species (D-band), always exists in those samples, irrespective of the carbonization, thus indicating incomplete graphitization of the nanotubes at such temperatures.

Figure 3 (bottom) shows UV/Vis spectra of the left-handed CPPy, CCNTs-550, and CCNTs-950 samples, which exhibit a broad absorption band in the range of 200–800 nm. On the basis of the chain structures and band models of PPy (see Figure S7 in the Supporting Information),[17] the bands at 230–320 nm and 340–400 nm could be assigned to the π-conjugated structure of pyrrole rings and interband π–π* transitions, respectively, and the intensity of these bands is thus directly proportional to the amount of neutral PPy. The band at about 500 nm represents a transition from the valence bond to the antibonding polaron or bipolaron state resulting from polaron absorption, the band at 680–800 nm or even higher wavelengths can be assigned to a transition from the valence bond to the bonding polaron or bipolaron state resulting from bipolaron absorption.[17] After heating to 550 °C, the increased intensity of the bands at 230–400 nm could be attributed to an increasing amount of the neutral form of PPy and pyridinic carbon.[17a] However, the decreased intensity of the bands at 680–800 nm could be assigned to partial destruction of the long-range π-conjugated structure of PPy chains as a result of carbonization.[17b] By heating to 950 °C, the samples are converted to partially graphitic carbon with the rearrangement of the structure. The amount of polarons and bipolarons decreases because of the intrachain rearrangement, which leads to the decrease in intensity of the bands at about 230–500 nm compared with those of CCNTs-550.[17] Nevertheless, the intensity of the bands still exceeds that of the as-prepared CPPy samples, which may be attributed to the higher conjugation and conductivity of sp^2-hybridized graphitic carbon compared with PPy rings. A similar effect was achieved for the sp^2-hybridized graphitic carbon chains, thus resulting in an increase in intensity of the bands at 680–800 nm.[17b,18] Moreover, both the increased number of sp^2-hybridized sites and the increased conductivity of the material cause a reduction in the gap width.[18] Thus, optical absorption at 230–500 nm shows a slight blue shift of the samples that were annealed at higher temperatures.

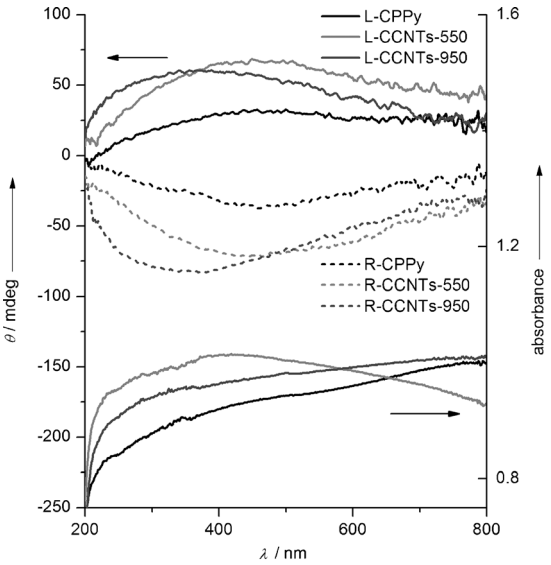

Figure 3. CD and UV/Vis spectra of enantiomeric CPPy nanotubes, CCNTs-550, and CCNTs-950.

Circular dichroism (CD) can be used to measure the differential absorption of left- and right-handed circularly polarized light, and the CD activity indicates a chiral structure, which can be detected by solid-state diffuse-reflectance circular dichroism (DRCD). The enantiomeric CPPy, CCNTs-550, and CCNTs-950 samples showed obvious mirror-imaged CD signals in the corresponding absorption region (Figure 3), thus indicating that the optically active carbonaceous tubes can selectively absorb left- or right-handed circularly polarized light through a vicinal effect of helically arranged polymer chains of PPy or the carbon nanostructure.[19] Additionally, their CD signals were slightly shifted to a lower wavelength with an increase of their intensity after carbonization, which is consistent with the change of optical absorption, as mentioned above.

On the other hand, the CCNTs also showed distinct electrochemical reactivity for lithium intercalation and may be potentially useful materials for lithium-ion batteries (LIBs). Figure 4a shows the discharge–charge curves of a CCNTs-950 electrode. The initial discharge capacity reaches 750 mAh g^{-1}. The voltage plateaus above 0.75 V in the first discharge curve can be attributed to the formation of a solid electrolyte interphase (SEI) film on the surface of the CCNTs, and other side reactions.[20] In the following cycles, the electrochemical reaction becomes reversible and voltage of lithium intercalation remains far above 0 V vs. Li^+/Li, which is favorable for safe battery operation. The cycling behavior of the CCNTs samples was further compared with that of commercial CNTs at 100 mA g^{-1}. The CCNTs-950 electrode

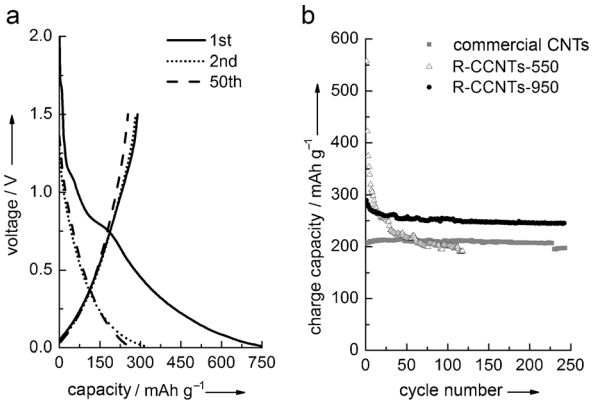

Figure 4. Electrochemical performances of CCNTs. a) 1st, 2nd, and 50th discharge and charge curves for the R-CCNTs-950 electrode at a current density of 100 mA g^{-1} and a voltage 0–2 V. b) Cycling behavior of R-CCNTs-550 and R-CCNTs-950, and commercial carbonaceous nanotubes (commercial CNTs).

has better cycling stability at the initial stage than the CCNTs-550 electrode (Figure 4b), which indicates fewer defects and a more stable structure of the CCNTs-950. Commercial CNTs (see Figure S8 in the Supporting Information), which have a specific surface area of 63 m^2 g^{-1} and a diameter of around 40 nm, show a reversible capacity of about 210 mAh g^{-1}, which is in accordance with the reported results.[21] Under the same conditions, the CCNTs-950 obviously have a higher capacity, which may be due to more open mesoporous channels in CCNTs and more active sites for lithium storage.[22]

To the best of our knowledge, this is the first example for the preparation of enantiopure chiral carbonaceous nanotubes with distinct optical activity through a one-step synthesis. The double-helical mesoporous PPy nanotubes were synthesized using N-acylamino acids as template and then easily carbonized to N-doped CCNTs and partially graphitized CCNTs with well-maintained helical morphology. All of these materials show obvious differential absorption of left- and right-handed circularly polarized light. As the mesoporous CCNTs with super-helical structure, they have shown higher lithium storage capacity compared with common CNTs. These new carbon materials with unique chiral configuration may have significant future applications in various research areas, such as in energy storage, as catalyst supports, and in enantioselective separation systems.

Experimental Section

Preparation of chiral PPy nanotubes: We modified a method previously reported by us,[9] using a molar ratio of 1:40:5351:57081:40 for lipid amphiphilic molecule/pyrrole/methanol/H_2O/ammonium persulfate (APS). C_{18}-D-Glu (0.06 mmol) was dissolved in MeOH (12.9 mL) at room temperature, and pyrrole (2.4 mmol) and deionized water (60 mL) were added. The solution was stirred for 10 min, then a precooled aqueous solution of APS (2.4 mmol in 1.2 mL deionized water) was added to the mixture, which was then stirred for further 30 min. A brown solid, which was obtained by filtration and thorough washing of the residue with H_2O and C_2H_5OH, was dried for 12 h at 40 °C in vacuum.

Carbonization of the CPPy nanotubes: The above-mentioned product were heated to the target temperature at a rate of 1.5 °C min^{-1} under a flow of Ar, and the temperature was maintained for 6 h. After slowly cooling the sample to room temperature, carbonized carbonaceous nanotubes were obtained.

Received: February 11, 2013
Published online: May 28, 2013

Keywords: carbon · chirality · nanotubes · polypyrrole · self-assembly

[1] a) K. E. Shopsowitz, H. Qi, W. Y. Hamad, M. J. MacLachlan, *Nature* **2010**, *468*, 422–425; b) A. Kuzyk, R. Schreiber, Z. Fan, G. Pardatscher, E.-M. Roller, A. Hogele, F. C. Simmel, A. O. Govorov, T. Liedl, *Nature* **2012**, *483*, 311–314; c) D. S. Su, *Angew. Chem.* **2011**, *123*, 4843–4847; *Angew. Chem. Int. Ed.* **2011**, *50*, 4747–4750; d) K. E. Shopsowitz, A. Stahl, W. Y. Hamad, M. J. MacLachlan, *Angew. Chem.* **2012**, *124*, 6992–6996; *Angew. Chem. Int. Ed.* **2012**, *51*, 6886–6890; e) C. Gautier, T. Bürgi, *ChemPhysChem* **2009**, *10*, 483–492; f) A. O. Govorov, Y. K. Gun'ko, J. M. Slocik, V. A. Gerard, Z. Fan, R. R. Naik, *J. Mater. Chem.* **2011**, *21*, 16806–16818; g) M. Yang, N. A. Kotov, *J. Mater. Chem.* **2011**, *21*, 6775.

[2] a) L. Hu, D. S. Hecht, G. Grüner, *Chem. Rev.* **2010**, *110*, 5790–5884; b) N. Karousis, N. Tagmatarchis, D. Tasis, *Chem. Rev.* **2010**, *110*, 5366–5397; c) D. Chen, L. Tang, J. Li, *Chem. Soc. Rev.* **2010**, *39*, 3157–3180.

[3] L. Xing, J. H. Xie, Y. S. Chen, L. X. Wang, Q. L. Zhou, *Adv. Synth. Catal.* **2008**, *350*, 1013–1016.

[4] D. K. Smith, *Chem. Soc. Rev.* **2009**, *38*, 684–694.

[5] C. Girardet, D. Vardanega, F. Picaud, *Chem. Phys. Lett.* **2007**, *443*, 113–117.

[6] a) X. Li, X. Tu, S. Zaric, K. Welsher, W. S. Seo, W. Zhao, H. Dai, *J. Am. Chem. Soc.* **2007**, *129*, 15770–15771; b) B. Wang, C. H. P. Poa, L. Wei, L. J. Li, Y. Yang, Y. Chen, *J. Am. Chem. Soc.* **2007**, *129*, 9014–9019; c) Y. Chen, L. Wei, B. Wang, S. Lim, D. Ciuparu, M. Zheng, J. Chen, C. Zoican, Y. Yang, G. L. Haller, *ACS Nano* **2007**, *1*, 327–336.

[7] a) G. Dukovic, M. Balaz, P. Doak, N. D. Berova, M. Zheng, R. S. Mclean, L. E. Brus, *J. Am. Chem. Soc.* **2006**, *128*, 9004–9005; b) X. Peng, N. Komatsu, S. Bhattacharya, T. Shimawaki, S. Aonuma, T. Kimura, A. Osuka, *Nat. Nanotechnol.* **2007**, *2*, 361–365.

[8] a) S. G. Telfer, N. Tajima, R. Kuroda, *J. Am. Chem. Soc.* **2004**, *126*, 1408–1418; b) M. Kasha, *Radiat. Res.* **1963**, *20*, 55–70.

[9] C. Fan, H. Qiu, J. Ruan, O. Terasaki, Y. Yan, Z. Wei, S. Che, *Adv. Funct. Mater.* **2008**, *18*, 2699–2707.

[10] a) T. Shimizu, M. Masuda, H. Minamikawa, *Chem. Rev.* **2005**, *105*, 1401–1444; b) S. Liu, L. Han, Y. Duan, S. Asahina, O. Terasaki, Y. Cao, B. Liu, L. Ma, J. Zhang, S. Che, *Nat. Commun.* **2012**, *3*, 1215.

[11] a) Y. Ma, S. Jiang, G. Jian, H. Tao, L. Yu, X. Wang, X. Wang, J. Zhu, Z. Hu, Y. Chen, *Energy Environ. Sci.* **2009**, *2*, 224–229; b) S. Shang, X. Yang, X. Tao, *Polymer* **2009**, *50*, 2815–2818.

[12] J. Casanovas, J. M. Ricart, J. Rubio, F. Illas, J. M. Jiménez-Mateos, *J. Am. Chem. Soc.* **1996**, *118*, 8071–8076.

[13] a) A. Zamudio, A. L. Elías, J. A. Rodríguez-Manzo, F. López-Urías, G. Rodríguez-Gattorno, F. Lupo, M. Rühle, D. J. Smith, H. Terrones, D. Díaz, M. Terrones, *Small* **2006**, *2*, 346–350; b) S. Jiang, Y. Ma, G. Jian, H. Tao, X. Wang, Y. Fan, Y. Lu, Z. Hu, Y. Chen, *Adv. Mater.* **2009**, *21*, 4953–4956.

[14] a) G. Cho, B. M. Fung, D. T. Glatzhofer, J. S. Lee, Y. G. Shul, *Langmuir* **2001**, *17*, 456–461; b) X. Zhang, J. Zhang, W. Song, Z. Liu, *J. Phys. Chem. B* **2006**, *110*, 1158–1165.

[15] a) P. M. Carrasco, H. J. Grande, M. Cortazar, J. M. Alberdi, J. Areizaga, J. A. Pomposo, *Synth. Met.* **2006**, *156*, 420 – 425; b) H. T. Ham, Y. S. Choi, N. Jeong, I. J. Chung, *Polymer* **2005**, *46*, 6308 – 6315; c) M. Forsyth, V. T. Truong, M. E. Smith, *Polymer* **1994**, *35*, 1593 – 1601.
[16] a) F. Tuinstra, J. L. Koenig, *J. Chem. Phys.* **1970**, *53*, 1126 – 1130; b) T. Kowalewski, N. V. Tsarevsky, K. Matyjaszewski, *J. Am. Chem. Soc.* **2002**, *124*, 10632 – 10633; c) T. Kyotani, N. Sonobe, A. Tomita, *Nature* **1988**, *331*, 331 – 333.
[17] a) R. Čabala, J. Škarda, K. Potje-Kamloth, *Phys. Chem. Chem. Phys.* **2000**, *2*, 3283 – 3291; b) X. G. Li, A. Li, M. R. Huang, Y. Liao, Y. G. Lu, *J. Phys. Chem. C* **2010**, *114*, 19244 – 19255.
[18] J. Robertson, *Adv. Phys.* **1986**, *35*, 317 – 374.
[19] a) R. F. Pasternack, C. Bustamante, P. J. Collings, A. Giannetto, E. J. Gibbs, *J. Am. Chem. Soc.* **1993**, *115*, 5393 – 5399; b) D. Keller, C. Bustamante, *J. Chem. Phys.* **1986**, *84*, 2972 – 2980.
[20] a) A. El Ruby Mohamed, S. Rohani, *Energy Environ. Sci.* **2011**, *4*, 1065 – 1086; b) Y. Zhang, G. Li, Y. Jin, Y. Zhang, J. Zhang, L. Zhang, *Chem. Phys. Lett.* **2002**, *365*, 300 – 304; c) L. Qie, W. Chen, Z. Wang, Q. Shao, X. Li, L. Yuan, X. Hu, W. Zhang, Y. Huang, *Adv. Mater.* **2012**, *24*, 2047 – 2050.
[21] Y. Zhang, T. Chen, J. Wang, G. Min, L. Pan, Z. Song, Z. Sun, W. Zhou, J. Zhang, *Appl. Surf. Sci.* **2012**, *258*, 4729 – 4732.
[22] a) A. R. Armstrong, C. Arrouvel, V. Gentili, S. C. Parker, M. S. Islam, P. G. Bruce, *Chem. Mater.* **2010**, *22*, 1759 – 1769; b) P. Simon, Y. Gogotsi, *Acc. Chem. Res.* **2013**, *46*, 1094 – 1103; c) Y. Ren, Z. Liu, F. Pourpoint, A. R. Armstrong, C. P. Grey, P. G. Bruce, *Angew. Chem.* **2012**, *124*, 2206 – 2209; *Angew. Chem. Int. Ed.* **2012**, *51*, 2164 – 2167; d) J. Ge, Y. Yin, *Angew. Chem.* **2011**, *123*, 1530 – 1561; *Angew. Chem. Int. Ed.* **2011**, *50*, 1492 – 1522.

